Ninth International Conference on
THIN-WALLED STRUCTURES – ICTWS2023
Sydney, Australia, Nov 29 – Dec 1, 2023

BENDING OF SANDWICH PANELS WITH VARIOUS CORES

Fukun Xia*, Yvonne Durandet*, PJ Tan, and Dong Ruan***

* Department of Mechanical and Product Design Engineering, School of Engineering, Swinburne University of Technology, Hawthorn, VIC3122, Australia
e-mails: fxia@swin.edu.au, ydurandet@swin.edu.au, druan@swin.edu.au

** Department of Mechanical Engineering, University College London, Torrington Place, London WC1E 7JE, UK
e-mail: pj.tan@ucl.ac.uk

Keywords: Corrugated sandwich panel; honeycomb; aluminum foam; truss sandwich panel; auxetics; bio-inspired structure.

Abstract. *In this paper, the bending performances of sandwich panels with corrugated triangular, honeycomb, aluminium foam, pyramidal truss, double sine corrugated (DSC), and 3D re-entrant auxetic cores are assessed and compared, both experimentally and numerically. Three-point bending experiments were performed on corrugated, honeycomb, aluminium foam, and truss core sandwich panels with identical face-sheets and core height. The experimental and numerical results compared well for panels with corrugated, honeycomb and truss cores. Parametric studies were subsequently performed, using ABAQUS, and three distinct modes of deformation were identified. The specific energy absorption (SEA) of the panels was found to increase with the core relative density; the one with a honeycomb core will be shown to have the greatest SEA, for the same core relative density, compared to the rests.*

1 INTRODUCTION

Sandwich panels consisting of a low-density core and thin skins (upper and lower) are widely used in applications that require a combination of high structural rigidity and lightweight, such as in aerospace, ships, and railway industry [1–4]. Compared to monolithic structures, these panels provide higher specific stiffness and strength-to-weight ratios. The sandwich cores often comprise corrugated and truss structures, honeycombs, and metal foams [5]. Below is a brief overview of the various core materials/types.

Metal foams, also known as stochastic foams (manufactured using a foaming route), have nearly isotropic mechanical properties. A metal foam core sandwich panel typically fails by face yielding, face wrinkling, core yielding, or local indentation [6].

A common feature of a prismatic honeycomb structure is its array of prismatic hollow cells separated by thin vertical walls. A honeycomb structure exhibits high out-of-plane compressive strength and shear properties, compared to its in-plane counterpart, at low density [7]. The failure mechanisms that develop under three-point bending include core shear, face yielding, face bending, indentation, and face wrinkling [8,9].

A truss core comprises struts organized into interconnected triangle units. The interior structure of a truss sandwich panel facilitates its multifunctional (e.g., crossflow heat exchange and shape morphing) applications [10]. Deshpande et al. [11] identified four competing failure mechanisms, viz. face yielding, face wrinkling, indentation, and core shear, where failure maps were constructed. Xiong et al. [12] investigated the bending performance of sandwich panels with pyramidal truss cores and carbon fiber composite face-sheets, where the failure mechanisms observed were face sheet crushing, face sheet wrinkling, core member buckling, and core crushing.

A corrugated core consists of plates or sheets with triangular, trapezoidal, or curvilinear shapes [13]. These sandwich panels are favored in many applications due to their ease of manufacturing, often through welding [14]. However, their bending performance varies with the loading direction due to anisotropy. Bending tests can be conducted along two principal directions relative to the corrugation axis: transverse (bending about an axis perpendicular to the corrugation axis) and longitudinal (bending about an axis parallel to the corrugation axis), as shown in Figure 1. Lu et al. [15] identified four failure mechanisms (face yielding, core yielding, face buckling, and core buckling) and derived a failure criterion for triangular corrugated sandwich panels under bending.

Bio-inspired structures have great potential as energy absorbers. Yang et al. [16] studied the uniaxial compression response of a sandwich panel whose double-sine corrugated core was arranged in a bio-inspired sinusoidal herringbone pattern. The sandwich panel with double-sine corrugated core was found to have greater energy absorption capacity and smaller initial peak force compared with triangular corrugated core sandwich panel.

Auxetic materials/structures exhibit negative Poisson's ratios and have excellent mechanical properties such as enhanced indentation resistance and energy absorption ability [17]. Chen et al. [18] has used auxetic structures as core of sandwich panel to study its blast response. The panel with auxetic core outperformed the one with hexagonal honeycomb core when the blast level was low, or the core relative density was high.

Hitherto, there are relatively few attempts to compare the bending performance of sandwich panels with different core types. Results from three-point bending experiments of sandwich panels with corrugated, truss, honeycomb and foam cores will be reported, and their performance (specific energy absorption) quantified and compared. Numerical models are developed, where their predictions were validated by the experimental data, and the former is used in a parametric study to elucidate the load-displacement curves and modes of deformation that develop during bending. Finally, their specific energy absorptions are quantified and compared.

2 EXPERIMENTS

2.1 Samples

The sandwich panels were manufactured by adhesively bonding two Al5005-H34 face-sheets to various core materials/types using Araldite 420 A/B epoxy adhesive. Subsequently, the samples were cured at 70 °C for two hours. All the samples have identical *x*-*z* plane dimensions of 200 mm × 50 mm, with an identical face-sheets thickness (t_f) of 1.0 mm and a core height (h_c) of 12.5 mm. Four types of sandwich core materials/types were investigated, viz. triangular corrugated, pyramidal truss, honeycomb, and aluminum foam.

Figure 1 (a) shows the longitudinal and transverse orientations of a corrugated sandwich panel, respectively. The two key geometric parameters of the corrugations are the web thickness, t_c, and corrugation angle, θ_c. Figure 1 (b) shows the schematic of a pyramidal truss core sandwich panel with strut thickness, t_t, strut width, w_t, and strut angle, θ_t (the angle between the strut and the lower face sheet). The honeycomb core was made from Al5052, where d_h and t_h are the cell size and cell wall thickness, respectively, as shown in Figure 1 (c). Figure 1 (d) shows an aluminum foam core sandwich panel, where the core was machined from a block of ALPORAS aluminum foam with a relative density ($\bar{\rho}$) of approximately 8%. Table 1 lists the geometric parameters, mass and material types for the different sandwich panels to be investigated here. Eight types of sandwich core, viz. Corrugated-T, Corrugated-L, Truss-A, Truss-B, Honeycomb-A, Honeycomb-B, Honeycomb-C, and Foam, were used experimentally.

The geometric configuration and dimensions for each are listed in Table 1. Three samples of each type were fabricated and tested.

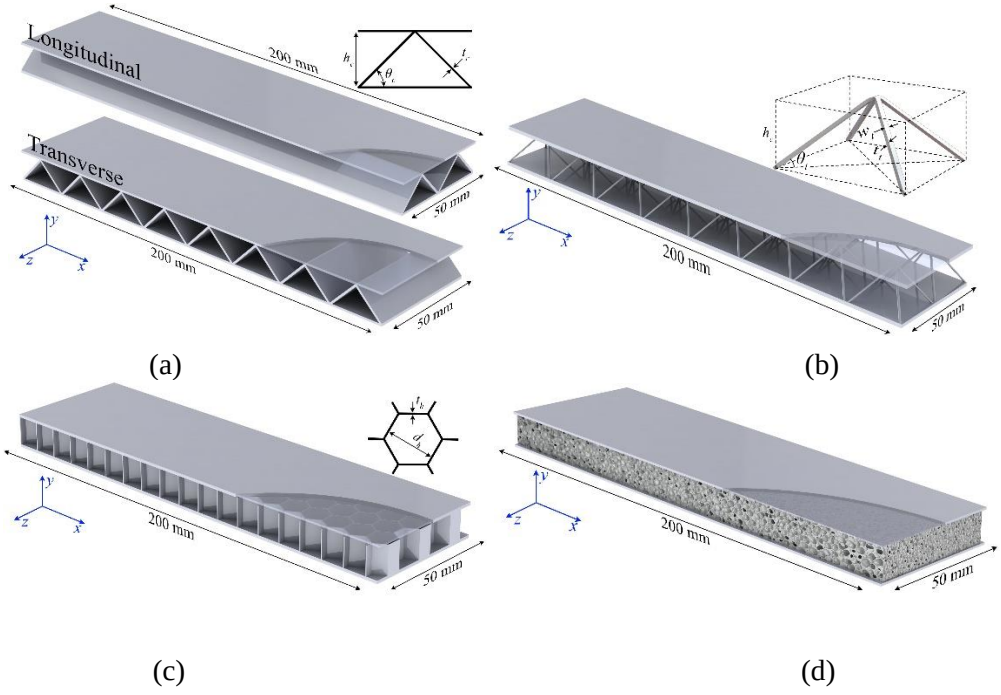

Figure.1. Schematics of the sandwich panel with (a) corrugated, (b) truss, (c) honeycomb, and (d) aluminium foam cores.

Table 1. Geometric configuration and dimensions of the sandwich panels

Sample	Orientation	t_c (mm)	θ_c (°)	Core material	Average mass (g)
Corrugated-T	Transverse	1.0	45	Al5005-H34	95.0
Corrugated-L	Longitudinal	1.0	45	Al5005-H34	95.3
	w_t (mm)	t_t (mm)	θt (°)		
Truss-A	2.0	0.6	35.26	Al5005-H34	59.7
Truss-B	2.0	1.0	35.26	Al5005-H34	62.7
	d_h (mm)	t_h (mm)			
Honeycomb-A	3.18	0.0254		Al5052	66.7
Honeycomb-B	3.97	0.0381		Al5052	67.7
Honeycomb-C	6.35	0.0762		Al5052	71.0
	$\bar{\rho}$				
Foam	8%			Al-Ca5-Ti3 [19]	86.1

2.2 Bending tests

Three-point bending experiments were performed on a 50 kN MTS machine (model 43) using a bending fixture (model FWA105A) at a loading rate of 1.5 mm/min. Three repeat tests were performed for each sandwich panel with a different core material/type. The loading pin/indenter and support rollers were made of high strength steel and had a diameter of 20 mm. The span between the two support rollers is l = 150 mm.

3 FINITE ELEMENT ANALYSIS (FEA)

Finite element (FE) simulations were performed using ABAQUS/Explicit. Panels with five different types of core materials/types were simulated: triangular corrugated core, pyramidal truss core, honeycomb core, double sine corrugated core (DSC), and 3D re-entrant auxetic core. However, the aluminum foam-core sandwich panel was not simulated in the parametric study due to a lack of precise material properties (such as failure strain) for different relative densities.

The material properties were tested and used in the FE models of the face-sheets and cores.. Both support rollers and the indenter were assumed to be rigid bodies. All degrees of freedom for the two support rollers were fixed, and the indenter is displaced in z-direction at a constant displacement rate of 50 mm/s - note that this is higher than in experiments - to reduce the computational time. Four-node shell elements (S4R) were used to mesh the face-sheets of the sandwich panels, including for the corrugated and honeycomb cores. The truss core and the rollers were meshed by two-node linear beam elements (B31) and four-node rigid elements (R3D4), respectively.

4 RESULTS AND DISCUSSIONS

4.1 Experimental and FE results

4.1.1 Corrugated core panel

Only one representative test result for the Corrugated-L and Corrugated-T panels is presented in Figure 2 (a) and (b), respectively, as the deformation mode observed in each repeated test is largely identical. The left images depict the experimental observations, while the right images show the corresponding numerical predictions obtained from FE simulations. Overall, the FE simulations successfully capture the deformation modes observed in the experiments. Both the Corrugated-L and Corrugated-T panels exhibit global bending and local indentation beneath the indenter. In the Corrugated-L panel, the corrugated core undergoes local bending due to interactions with the top face-sheet that intrudes into the core space.

The load-displacement curves of the corrugated sandwich panels subjected to transverse and longitudinal bending are shown in Figure 2(c) and (d), respectively. The peak load of a Corrugated-L panel is approximately six times higher than its Corrugated-T counterpart. This is unsurprising since, in the former, the intrusion by the top face sheet is resisted by all the corrugations along the x-direction, unlike the latter. In general, the FE model successfully captures the general trend of the load-displacement curve obtained experimentally.

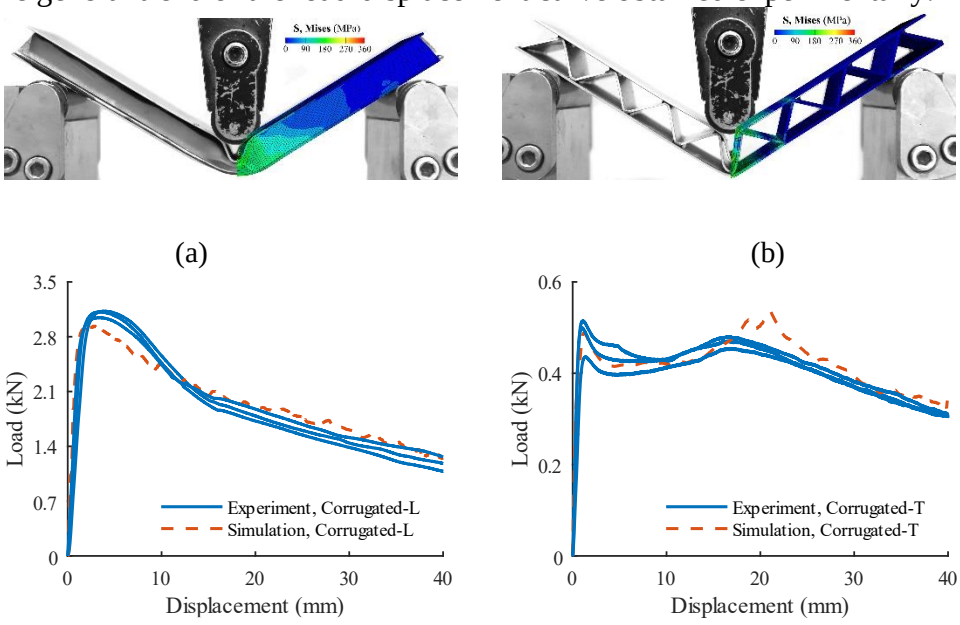

Figure. 2. Comparison between experimental and numerical results: (a) Corrugated-L panel; (b) Corrugated-T panel; (c) load-displacement curves of Corrugated-L panels; and, (d) load-displacement curves of Corrugated-T panels.

4.1.2 Truss core panel

Two deformation modes were observed for the Truss-A panel. As shown in Figure 3 (a), all the core struts on the left side of the panel had collapsed. By contrast, this only occurred for those core struts next to the indenter on the right. This asymmetric deformation was induced because the indenter was not positioned exactly at the mid-point of the panel in the experiments - the offset was approximately 1 mm. The FE simulation (Simulation 1) also predicts an asymmetric deformation at the same offset. Figures 3 (b) and (c) shows a Truss-A panel that deformed symmetrically when indenter is placed at the mid-point of the. Figure 3 (c) shows that a Truss-B panel exhibits similar symmetric deformation to that of Truss-A. However, the region of local indentation is smaller in Truss-B due to its stronger core (higher t_t).

Three experimental and two FE-predicted load-displacement curves are plotted in Figure 3 (d). The peak load in both experiments and numerical predictions are approximately 0.35 kN. The average load after the indenter displacement of 10 mm in simulations is slightly higher than those in experiments. If there is offset of the indenter, two of the experimental curves and the curve of Simulation 1 fluctuate severely until the indenter displacement reaches approximately 10 mm. By contrast, the curves without offset of the indenter is less than 5 mm, which corresponds to the collapse of the two cells beneath the indenter.

The load-displacement curve of the Truss-B panel showed less fluctuations. The thicker core struts provide stronger support to the face-sheets. In these experiments, the top face-sheets contacted the adhesive on the bottom face-sheet at the indenter displacement of 30 mm, after which the force increased. The simulated load has a similar peak and overall trend. However, the higher simulated load when the indenter displacement is from 10 mm to 20 mm and the lower simulated one after the indenter displacement of 30 mm may be caused by the manufacturing error and adhesive.

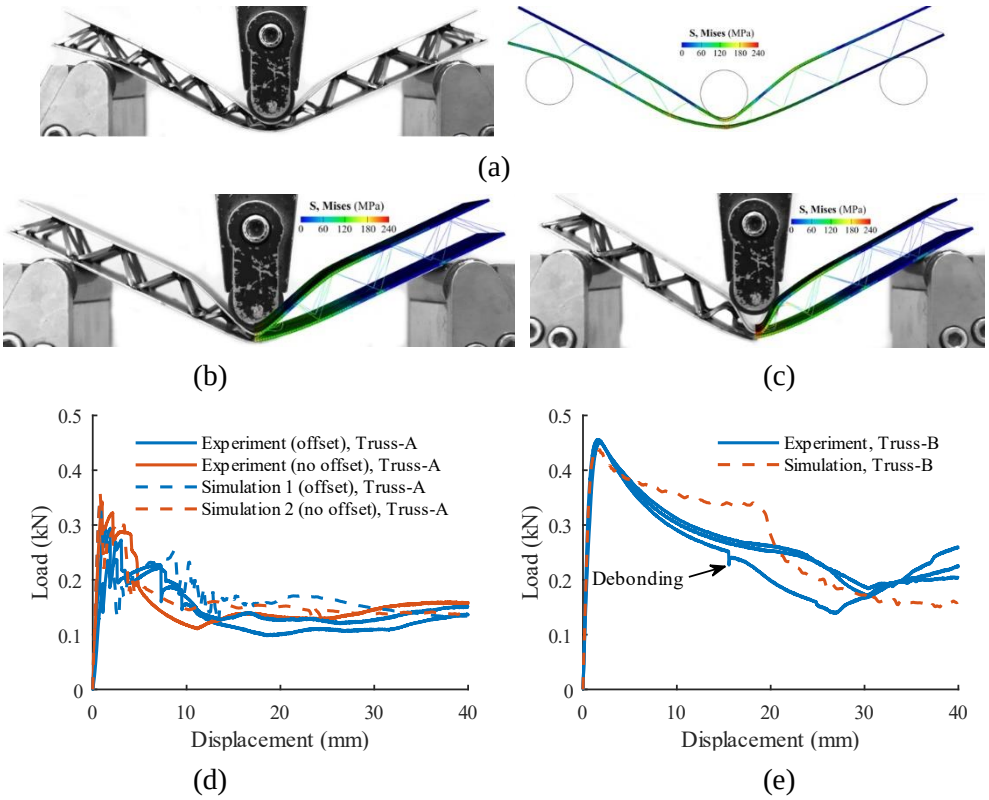

Figure. 3. Comparison between experimental and numerical results: (a) Truss-A panel when indenter was 1 mm away from the middle of the panel; (b) Truss-A panel when the indenter was in the middle of the panel; (c) Truss-B panel; (d) load-displacement curves of samples Truss-A panels; and, (e) load-displacement curves of samples Truss-B.

4.1.3 Honeycomb core panel

Honeycomb-A, Honeycomb-B, and Honeycomb-C have a similar deformation mode – global bending along with a narrow region of deep local indentation – which is seen in both experiments and FE simulations (see Figures 4a-c). Only a very small portion of the core under the indenter was crushed. The same deformation mode was also reported in [16] and [17]. In the study of Sun et al. [17], the deformation mode shown in Figs. 8 (a)-(c) was denoted as Mode A, in which a void occurred underneath the indenter due to the deformation of the top face-sheet. In the other mode (Mode B), the indenter was in full contact with the deformed top face-sheet. The panels with thinner skin and greater honeycomb cell size tend to deform in Mode A

The predicted load-displacement curves (see Figures 4d-e) by FE match reasonably well with their corresponding experimental one - the peak loads are 1.37 kN, 1.79 kN, and 2.10 kN. The differences of experimental and simulated loads in the initial stage maybe because of the adhesive layer in experiments. The tie connection between the core and face-sheets in simulation was stronger than the adhesive bonding in experiments. Honeycomb-A has the lowest peak load (1.38 kN for both experiments and simulation) since it has the weakest core, followed by Honeycomb-B (1.81 kN for experiments and 1.62 kN for simulation) and Honeycomb-C (2.08 kN for experiments and 1.94 kN for simulation) whose core relative density is the highest of the three.

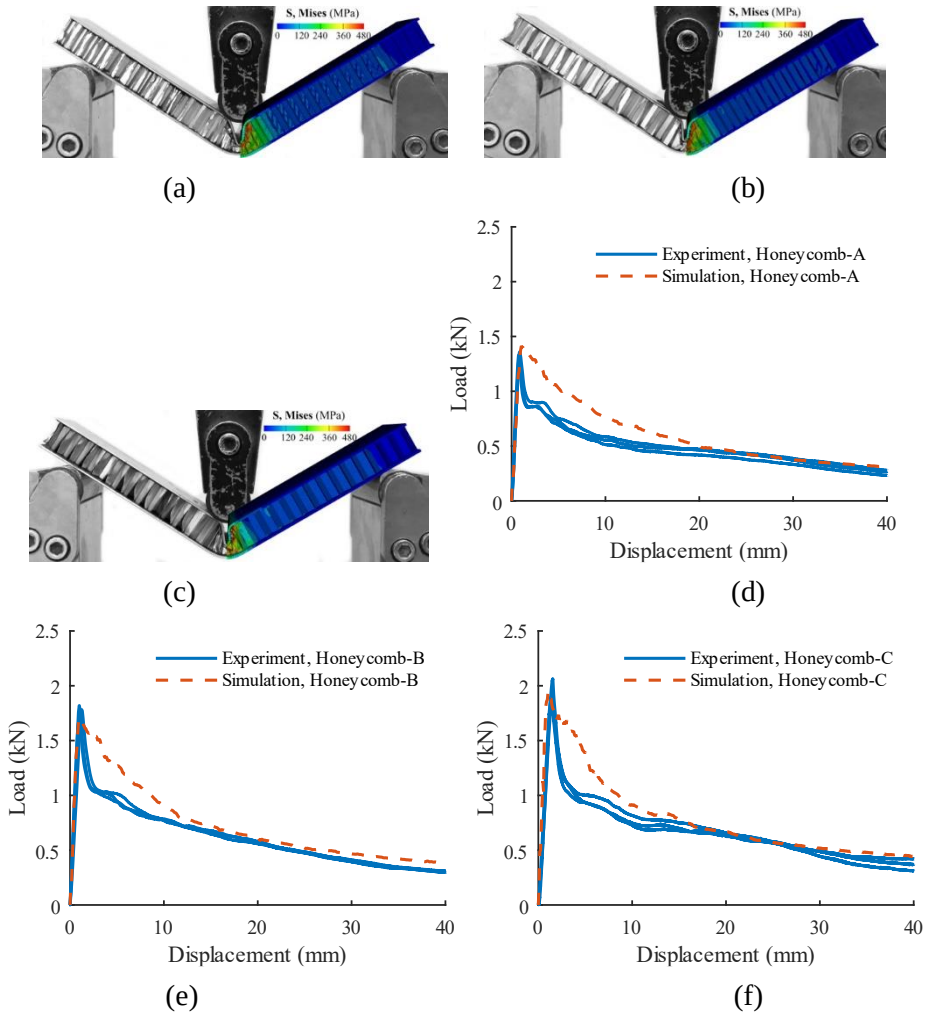

Figure 4. (a), (b), and (c) are the experimental (left image) and numerical (right image) deformation modes for Honeycomb-A, Honeycomb-B, and Honeycomb-C panels, respectively. Their corresponding load-displacement curves are shown in (d), (e), and (f), respectively.

4.1.4 Aluminum foam core panel

Core shear failure occurred in the foam core panels, as shown in Figures 5(a), (b), and (c). Plastic hinges developed along two sections of the panel – one beneath the indenter, and the other close to one of the supports (shown by the red dots in Figure 5(a). This asymmetric deformation mode is similar to Mode II deformation mode observed by Crupi et al. [8], which tends to occur in the experiments with the smaller span of supports. Figure 5 (d) shows the load-displacement curves of the panels. The sharp drops in the load-displacement curves are caused by the shear damage of the core (highlighted in the blue ovals).

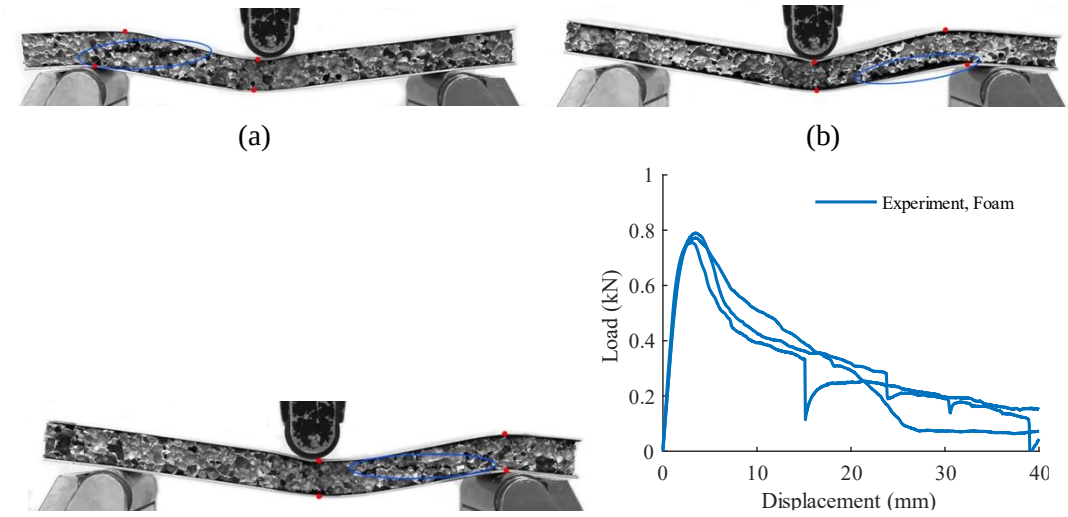

Figure 5. Experimental results of aluminum foam sandwich panels: (a), (b), and (c) are the deformations of the panels when the indenter displacement is 10 mm; (d) load-displacement curves.

4.2 Parametric study

Figures 2, 3, and 4 show a good agreement between FE predictions and experimental results, both in terms of the deformation mode and load-displacement curve. The validated numerical models are now employed to perform parametric study for the corrugated, truss and honeycomb core panels. In the parametric study, the core material and face-sheets are assumed to be made from Al5005-H34. Some of the geometric parameters for the panels are fixed, viz. face-sheet thickness is 1.0 mm, core height is 12.5 mm, the span between the two support pins is 150 mm, and the diameter of support pins and indenter is 20 mm. Aluminum foam sandwich panel is not considered due to a lack of an accurate material constitutive model.

Two additional sandwich panels with double-sine corrugated (DSC) core and auxetic core, are simulated here. The double-sine corrugated (DSC) core was meshed by three-node shell elements (S3) as shown in Figure 6 (a). The appropriate mesh size was determined from a mesh convergency study. The double-sine corrugated core can be expressed by the following Equation 1, where, x and z axes are the two in-plane directions, and y-axis is the out-of-plane direction. A is the out-of-plane amplitude of the wave, which is 12.5 mm for all the panels. λ is the wavelength. Two full waves are introduced along the width of the panel (in the z-direction). The other geometric parameter is core thickness (t_d). Base and node indentations are also considered for the bending of double-sine corrugated sandwich panel, shown schematically in Figure 6 (b).

$$Y(x,z) = A\sin\frac{2\pi x}{\lambda}\sin\frac{2\pi z}{\lambda} \tag{1}$$

The 3-D re-entrant auxetic core is shown in Figure 6(c). The geometric parameters of the auxetic core cell are the height of the vertical strut (h_a), the length of the re-entrant strut (l_a), the angle between the vertical strut and oblique strut (θ_a), and the edge length of the strut cross section (t_a). There is only one cell along the out-of-plane direction (y-direction) of the auxetic core. Therefore, the geometric parameters should satisfy the following relationship:

$$2h_a - 2l_a\cos\theta_a = h_c \tag{2}$$

where h_c is the core height and is 12.5 mm. Also, $h_a = 2l_a$ in the parametric study. Therefore, only two parameters, viz. θ_a and t_a, are varied. The geometric parameters of all the sandwich panels investigated in this section are listed in Tables 2 to 6.

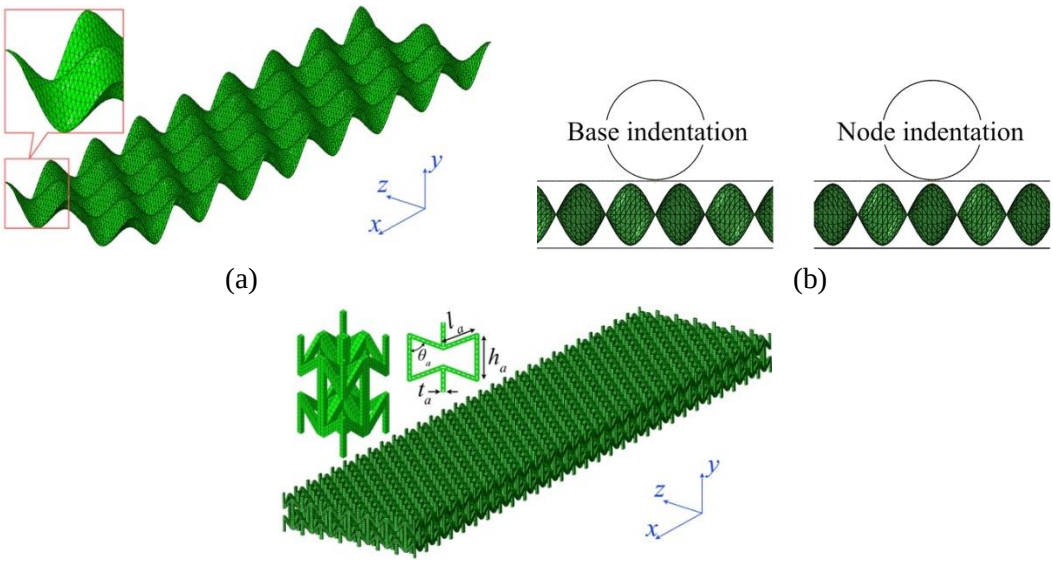

(a) (b)

(c)

Figure 6. Finite element model of the (a) double-sine corrugated core; (b) base indentation and node indentation of the panels with DSC core; (c) 3D re-entrant auxetic core.

Table 2. Geometric parameters of the sandwich panels with corrugated core

Sample	C-1	C-2	C-3	C-4	C-5	C-6	C-7	C-8	C-9
t_c (mm)	0.3	0.3	0.3	0.6	0.6	0.6	1.0	1.0	1.0
θ_c (°)	30	45	60	30	45	60	30	45	60

Table 3. Geometric parameters of the sandwich panels with truss core

Sample	T-1	T-2	T-3	T-4	T-5	T-6	T-7	T-8	T-9
w_t (mm)	0.3	0.3	0.3	0.6	0.6	0.6	1.0	1.0	1.0
θ_t (°)	22.2	35.3	50.8	22.2	35.3	50.8	22.2	35.3	50.8

Table 4. Geometric parameters of the sandwich panels with honeycomb core

Sample	H-1	H-2	H-3	H-4	H-5	H-6	H-7	H-8	H-9
d_h (mm)	3.18	3.18	3.18	3.97	3.97	3.97	6.35	6.35	6.35
t_h (mm)	0.0254	0.0381	0.0762	0.0254	0.0381	0.0762	0.0254	0.0381	0.0762

Table 5. Geometric parameters of the sandwich panels with DSC core

Sample	D-1	D-2	D-3	D-4	D-5	D-6
λ	15	15	20	20	25	25
t_d (mm)	0.25	0.5	0.25	0.5	0.25	0.5

Table 6. Geometric parameters of the sandwich panels with auxetic core

Sample	A-1	A-2	A-3	A-4	A-5	A-6
t_a (mm)	0.5	0.5	0.5	1.0	1.0	1.0
θ_a (°)	30	45	60	30	45	60

Three distinct deformation modes were observed in the investigated panels. The first mode involves global bending and local indentation. Plastic hinges form in the middle of the top face-sheet, compressing the core significantly. The load peaks before dropping dramatically due to core cell bending, and then stabilizes or decreases further. The second mode is characterized by global bending and uniaxial crushing, more common in low-density core corrugated and truss panels, showing severe load fluctuations. The third mode, exclusive to auxetic sandwich panels, exhibits rapid load rise without localized indentation beneath the indenter.

To assess the energy absorption ability of the different panels, their specific energy absorption (SEA) – this is defined as the energy absorbed per unit mass of the panel - is calculated. The absorbed energy is the area under the load-displacement curve between the indenter displacement of 0 to 40 mm. In the calculation of the SEA, only the mass of the panel between the supports is considered.

Figure 7 shows the SEA vs. relative density of all sandwich panel cores in the study. Higher core relative density generally corresponds to greater SEA for all panels. Corrugated panels' SEA increases with relative density, but not monotonically due to different deformation modes. Truss panels' SEA increases consistently with core relative density. Lower λ and higher t_d in DSC core panels result in greater SEA. For auxetic panels, larger ta leads to higher SEA, but at the same t_a, the panel with θ_a of 45° has the lowest SEA.

Comparing panels with identical core relative density, the honeycomb core panel has the highest SEA. The lowest SEA is observed in panels with corrugated core under transverse bending and auxetic core. However, corrugated core panels under longitudinal bending and DSC core panels show similar SEA. The auxetic sandwich panel exhibits relatively low SEA but displays a desirable load-displacement curve for energy absorption. Panels under node indentation generally have higher SEA compared to those under base indentation. Moreover, corrugated core panels have higher SEA under longitudinal bending than under transverse bending, with this difference increasing with the relative density's rise.

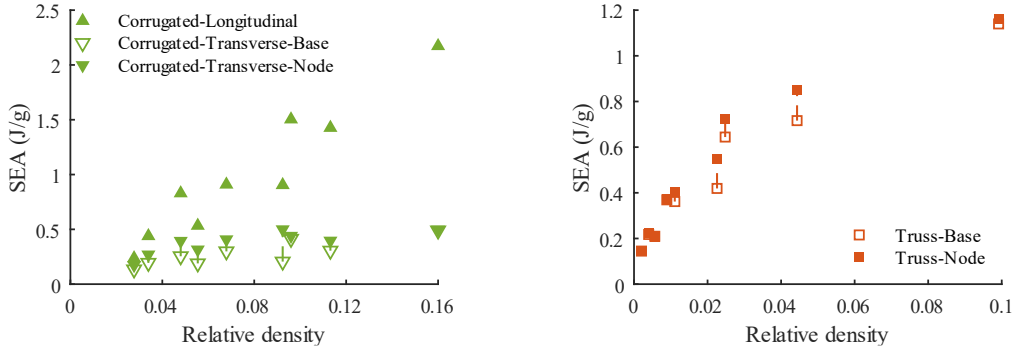

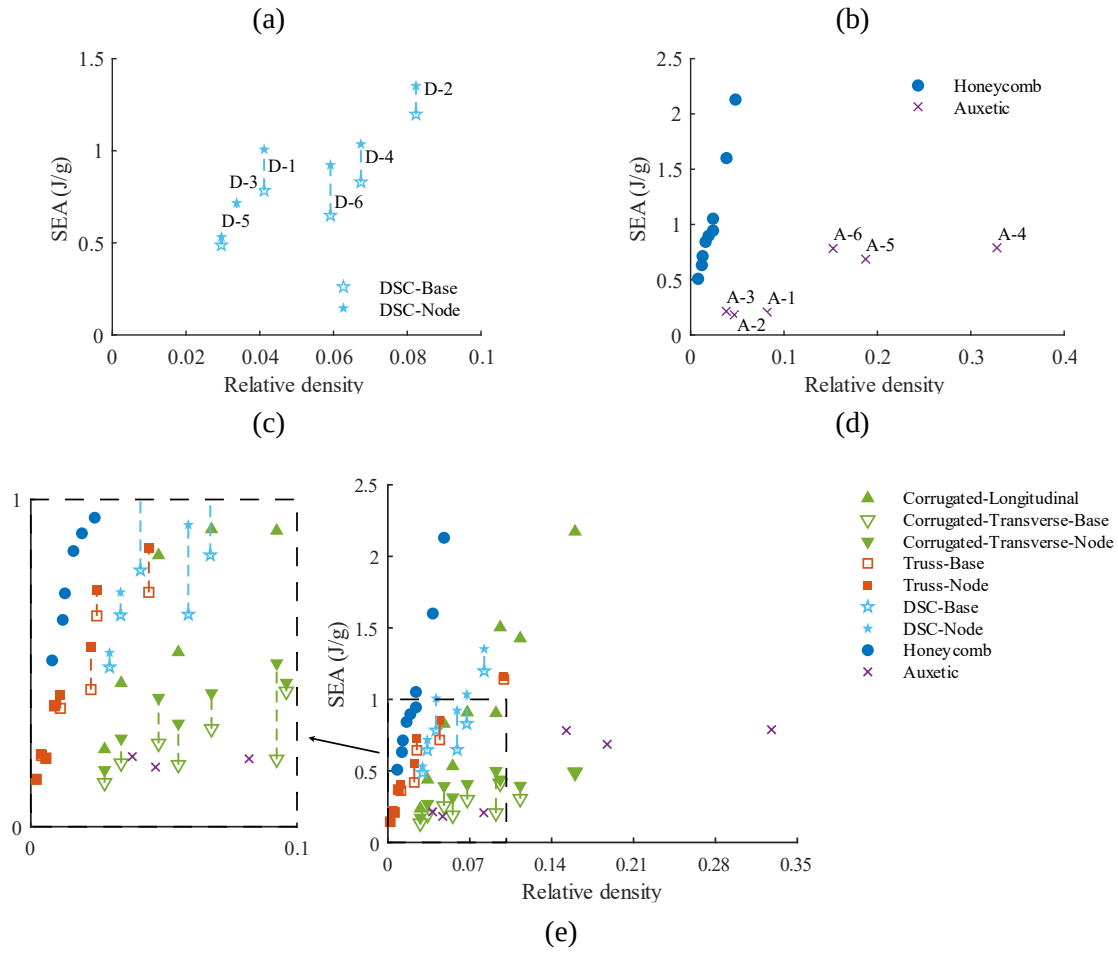

Figure 7. SEA vs. relative density of the (a) corrugated, (b) truss, (c) DSC, (d) honeycomb and auxetic cores, and (e) is the comparison for all core types.

5 CONCLUSIONS

Three-point bending performance of sandwich panels with triangular corrugated core, pyramidal truss core, honeycomb core, aluminum foam core, double sine corrugated core (DSC), and 3D re-entrant auxetic core was studied and compared. Experiments were firstly conducted on the corrugated, truss, honeycomb, and foam core sandwich panels. Most of the panels experienced global bending and local indentation. Subsequently, parametric study was performed using the validates numerical models. The DSC and auxetic sandwich panels along with the panels in experiments except for foam sandwich panel were included in the parametric study. Three deformation modes and load-displacement trends were observed. In all types of sandwich panels, the SEA tended to increase with the increase of the relative density of the core. Within the range of parameters studied, when the relative density was the same, honeycomb sandwich panel had the greatest SEA, and the panel with corrugated (transverse loading) and auxetic core had the lowest SEA.

REFERENCES

[1] Harris C.E., Starnes J.H. and Shuart M.J., "An assessment of the state-of-the-art in the design and manufacturing of large composite structures for aerospace vehicles", *NASA Technical Memorandum*, **39**, 1–24, 2001.

[2] Metschkow B., "Sandwich panels in shipbuilding", *Polish Maritime Research*, 5–8, 2006.

[3] Wahrhaftig, A., Ribeiro, H., Nascimento, A. and Filho, M., "Analysis of a new composite material for watercraft manufacturing", *Journal of marine science and application*, ***15***, 336-342, 2016.

[4] Kim, J.S., Lee, S.J. and Shin, K.B., "Manufacturing and structural safety evaluation of a composite train carbody", *Composite structures*, **78**(4), 468-476, 2007

[5] Zhu, F., Lu, G., Ruan, D. and Wang, Z., "Plastic deformation, failure and energy absorption of sandwich structures with metallic cellular cores", *International Journal of Protective Structures*, **1**(4), 507-541, 2010.

[6] McCormack, T.M., Miller, R., Kesler, O. and Gibson, L.J., "Failure of sandwich beams with metallic foam cores", *International Journal of Solids and Structures*, **38**(28-29), 4901-4920, 2001.

[7] Wahl, L., Maas, S., Waldmann, D., Zürbes, A. and Frères, P., "Shear stresses in honeycomb sandwich plates: Analytical solution, finite element method and experimental verification", *Journal of Sandwich Structures & Materials*, **14**(4), 449-468, 2012.

[8] Menta, V.G.K., Vuppalapati, R.R., Chandrashekhara, K., Pfitzinger, D. and Phan, N., "Manufacturing and mechanical performance evaluation of resin-infused honeycomb composites", *Journal of Reinforced Plastics and Composites*, **31**(6), 415-423, 2012.

[9] Crupi, V., Kara, E., Epasto, G., Guglielmino, E. and Aykul, H., "Theoretical and experimental analysis for the impact response of glass fibre reinforced aluminium honeycomb sandwiches", *Journal of Sandwich Structures & Materials*, **20**(1), 42-69, 2018.

[10] Kooistra, G.W., Queheillalt, D.T. and Wadley, H.N., "Shear behavior of aluminum lattice truss sandwich panel structures", *Materials Science and Engineering: A*, **472**(1-2), 242-250, 2008.

[11] Deshpande, V.S. and Fleck, N.A., "Collapse of truss core sandwich beams in 3-point bending", *International Journal of Solids and Structures*, **38**(36-37), 6275-6305, 2001.

[12] Xiong, J., Ma, L., Pan, S., Wu, L., Papadopoulos, J. and Vaziri, A., "Shear and bending performance of carbon fiber composite sandwich panels with pyramidal truss cores", *Acta Materialia*, **60**(4), 1455-1466, 2012.

[13] Dahiwale, N.B., Panigrahi, S.K. and Akella, K., "Numerical analyses of sandwich panels with triangular core subjected to impact loading", *Journal of Sandwich Structures & Materials*, **17**(3), 238-257, 2015.

[14] Côté, F., Deshpande, V.S., Fleck, N.A. and Evans, A.G., "The compressive and shear responses of corrugated and diamond lattice materials", *International Journal of Solids and Structures*, **43**(20), 6220-6242, 2006.

[15] Lu, T.J., Hutchinson, J.W. and Evans, A.G., "Optimal design of a flexural actuator", *Journal of the Mechanics and Physics of Solids*, **49**(9), 2071-2093, 2001.

[16] Yang, X., Ma, J., Shi, Y., Sun, Y. and Yang, J., "Crashworthiness investigation of the bio-inspired bi-directionally corrugated core sandwich panel under quasi-static crushing load", *Materials & Design*, **135**, 275-290, 2017.

[17] Wang, X.T., Wang, B., Li, X.W. and Ma, L., "Mechanical properties of 3D re-entrant auxetic cellular structures", *International Journal of Mechanical Sciences*, **131**, 396-407, 2017.

[18] Chen, G., Zhang, P., Deng, N., Cai, S., Cheng, Y. and Liu, J., "Paper tube-guided blast response of sandwich panels with auxetic re-entrant and regular hexagonal honeycomb cores–An experimental study", *Engineering Structures*, **253,** 113790, 2022.

[19] Yahaya, M.A., Ruan, D., Lu, G. and Dargusch, M.S., "Response of aluminium honeycomb sandwich panels subjected to foam projectile impact–An experimental study", *International Journal of Impact Engineering*, **75**, 100-109, 2015.